IEEE Access
Multidisciplinary | Rapid Review | Open Access Journal

Received March 19, 2018, accepted April 21, 2018, date of publication April 27, 2018, date of current version May 24, 2018.

Digital Object Identifier 10.1109/ACCESS.2018.2830768

Dynamic Optimal Control of a One-Dimensional Magnetohydrodynamic System With Bilinear Actuation

ZHIGANG REN[1,2], (Member, IEEE), ZHIJIA ZHAO[3], ZONGZE WU[1,2], (Member, IEEE), AND TEHUAN CHEN[4]

[1]School of Automation, Guangdong University of Technology, Guangzhou 510006, China
[2]Guangdong Key Laboratory of IoT Information Technology, Guangdong University of Technology, Guangzhou 510006, China
[3]School of Mechanical and Electrical Engineering, Guangzhou University, Guangzhou 510006, China
[4]Faculty of Mechanical Engineering and Mechanics, Ningbo University, Ningbo 315211, China

Corresponding author: Zongze Wu (zzwu@gdut.edu.cn)

This work was supported in part by the National Natural Science Foundation of China under Grant 61703114, Grant 61673126, and Grant 61703217, in part by the Science and Technology Plan Project of Guangdong under Grant 2014B090907010 and Grant 2015B010131014, and in part by the Innovative School Project of Education Department of Guangdong under Grant 2017KQNCX153, 2017KZDXM060.

ABSTRACT The manipulation of the magnetic field has been a proven effective method to change the flow velocity in magnetohydrodynamics (MHD) flow systems. In this paper, we consider a novel bilinear magnetic control problem arising in a 1-D MHD flow system modeled by a set of coupled partial differential equations (PDEs). We formulate the control of the magnetic field as a finite-time PDE-constrained dynamic optimal control problem and our aim is to realize the desired stationary state of the flow velocity at a specific terminal time. A model order reduction technique, based on proper orthogonal decomposition and Galerkin projection procedure, is first adopted to approximate the original complex optimization problem governed by PDEs into a semi-discrete approximation problem governed by a low-dimensional reduced-order model, and therefore can efficiently reduce the computational burden of the dynamic system. Then, the piecewise-linear control parameterization method is used to obtain an approximate optimal parameter selection problem that can be solved using nonlinear optimization techniques such as sequential quadratic programming. The exact formulas for the gradients of the defined cost functional with respect to the decision parameters are analytically derived via state sensitivity method. Numerical simulation results verify the effectiveness of our proposed computational method. The methodology proposed in this paper is a potential implementation of a real-time control strategy in a number of MHD flow systems.

INDEX TERMS Distributed parameter systems, PDE-constrained optimization, control parameterization, Galerkin projection, proper orthogonal decomposition (POD), MHD flow.

I. INTRODUCTION

In various natural physical phenomena and engineering problems, i.e., heat and diffusion procedures [1]–[3], flow fluid [4], [5], flexible structure systems [6]–[11] and plasma transport processes [12]–[14], one can find that the dynamic behaviors of these systems are not only related with the temporal evolution, but also related with the spatial evolution. These spatial-temporal evolutionary processes are usually mathematically modeled by a set of partial differential equations (PDEs), which are also commonly referred to as distributed parameter systems (DPS). As an important type of DPS, the magnetohydrodynamics (MHD) flow system, whose dynamics can be mathematically modeled by a set of Navier-Stokes PDEs and Maxwell equations, is generally characterized by an electrically conducting fluid moving between parallel plates in the presence of an external imposed magnetic and electric fields (See Fig. 1) [15]. In an MHD flow system, the movement of the conducting fluid between the parallel plates will produce an electric field and subsequently an electric current. Due to these natures, MHD flow has been covered numerous applications (e.g., [15]–[20]). Seeking efficient control strategies for the MHD flow system has attracted considerable attention in recent years.

In this paper, we consider a one-dimensional (1-D) incompressible, Newtonian MHD flow system, whose dynamic is controlled by an external induction of the magnetic field.

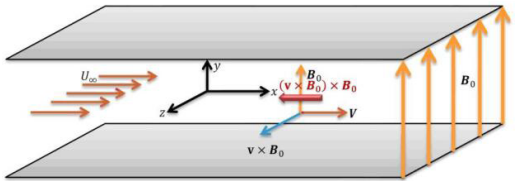

FIGURE 1. Sketch of a 3-D MHD flow.

The mathematical model of the 1-D MHD flow system studied in this paper is formulated as the following dimensionless form [21]:

$$\begin{cases} \dfrac{\partial u(l,t)}{\partial t} = \nu \dfrac{\partial^2 u(l,t)}{\partial l^2} + \varrho(t)\dfrac{\partial B(l,t)}{\partial l} - p(t), & \text{(1a)} \\ \dfrac{\partial B(l,t)}{\partial t} = \nu_m \dfrac{\partial^2 B(l,t)}{\partial l^2} + \varrho(t)\dfrac{\partial u(l,t)}{\partial l}, & \text{(1b)} \\ u(0,t) = 0, \quad u(1,t) = 0, & \text{(1c)} \\ B(0,t) = 0, \quad B(1,t) = 0, & \text{(1d)} \\ u(l,0) = u_0(l), \quad B(l,0) = B_0(l), & \text{(1e)} \end{cases}$$

where $t \in [0, T]$ denotes the time; $l \in [0, 1]$ denotes the space variable; $u(l, t)$ and $B(l, t)$ denote the flow velocity and the magnetic induction, respectively; $p(t)$ is the pressure difference per unit of the channel length; $\nu = 1/Re$ and $\nu_m = 1/Re_m$, Re is the flow Reynolds number and Re_m is the magnetic Reynolds number. In our current work, we assume the ranges of the coefficients ν and ν_m in (1) are small constants ranging from 0.01 to 10. The function $\varrho(t)$, which is the induction of the external magnetic field, is considered as the control input and satisfied the following physical constraint:

$$0 \le \varrho(t) \le \varrho_{max}, \tag{2}$$

where $\varrho_{\max}$ denotes the maximum magnetic filed.

The dynamic coupled PDEs (1) described above represents a typical class of MHD flow systems, and in PDE system (1), the flow velocity and electromagnetic fields are tightly coupled. The velocity in the MHD flow is also perpendicular to the magnetic vector. Besides, in the 1-D MHD flow system, the boundary conditions are zeros, which denote the velocity of the viscous fluid and the magnetic field corresponding to the continuity of the magnetic field strength on the parallel solid surfaces are zeros, respectively. In the past decades, various dynamic models of MHD flow systems which are based on boundary control inputs have been well investigated in the literature [4], [5], [22], [23]. Other recent developments about the modeling and control of the MHD flow systems have also been investigated [24], [25]. Compared to these boundary control problems of MHD flow such as in prior works [4], [5], [22], [23], the significant characteristic of the system (1) studied in this paper is that the external control input (external induction of magnetic field) is taken multiplicative effect exerted on momentum and magnetic components of the system variables. The MHD flow system (1) is thus so-called a bilinear control PDEs system, and to our best knowledge, there are very few works of literature studied with such a spirit.

In this paper, we focus on solving an optimal bilinear control problem governed by the PDE system (1). The tracking control of the desired stationary state of the flow velocity at a specific terminal time in the 1-D MHD flow is formulated as a dynamic optimal control problem. Our aim is to design an optimal controller $\varrho(t)$ to drive the flow velocity $u(l, t)$ to within close proximity of the stationary state of the desired flow velocity (i.e., $u(l, T) = 0$) at the pre-indicated terminal time T. Different with various existing control strategies successfully applied in infinite dimensional systems [4], [19], [26]–[30], it is a very challenging task to provide analytic optimal strategies for such coupled MHD flow system (1) involving bilinear control. Thus, computational optimal control algorithms for the solution of these PDEs arise an effective alternative. However, due to the high dimensionality and complexity of the original coupled PDEs, i.e., required a large computation time for solving the PDEs numerically, it is often hard to use the PDE model directly to analyze and control the system in real-time. One most effective way in real applications is to first reduce the original PDE model to a lower dimensional dynamic system governed by an ordinary differential equation (ODE) model. This procedure is well known as reduced order modeling (ROM) techniques. The proper orthogonal decomposition (POD) method is an efficient ROM technique of obtaining the lower finite dimensional dynamical systems from the data ensembles arising from experimental observation or numerical simulations of high-dimensional systems, and it has been successfully applied in many areas [31]–[33]. In present work, we first use the POD method combined the Galerkin projection to reduce the original PDEs system (1) to a low order dynamic system modeled by ODEs, leading to a more simple real-time optimal control problem for the MHD flow system. Then, we use the piecewise-linear control parameterization method to approximate the control input by a linear combination of temporal basis functions with the constant coefficients to be determined by the numerical optimization procedures such as sequential quadratic programming (SQP). The exact formulas for the gradients of the defined cost function with respect to the decision parameters are analytically derived via state sensitivity method. Based on the obtained gradient formulas, the gradient-based optimization method is used to obtain the optimal solutions. Numerical simulation results verify the effectiveness of our proposed computational method. The main contribution of this paper is that we develop an effective computational optimal control method based on POD method and control parameterization method to realize the optimal target of the stationary state of the flow velocity arising in a novel bilinear controlled 1-D MHD flow system, and this methodology proposed in this paper is potential implementation of a real-time receding-horizon control strategy in future.

The rest of this paper is organized as follows. In Section II, we propose the bilinear optimal control problem for the 1-D MHD flow system. In Section III, we use the

POD method combined with the Galerkin projection to obtain a lower finite-dimensional model derived from the original coupled PDEs. In Section IV, we give the detailed procedure of the optimal control computation which is based on piecewise-linear control parameterization. The gradients of the cost function are derived analytically. In Section V, the numerical results for the 1-D MHD flow system are presented. Finally, the paper is closed in Section VI by summarizing our results and research topics.

Notations: $u_t(l,t) = \partial u(l,t)/\partial t$, $u_l(l,t) = \partial u(l,t)/\partial x$, $u_{ll}(l,t) = \partial^2 u(l,t)/\partial l^2$, $B_t(l,t) = \partial B(l,t)/\partial t$, $B_l(l,t) = \partial B(l,t)/\partial l$, $B_{ll}(l,t) = \partial^2 B(l,t)/\partial l^2$, $< f(l), g(l) >= \int_0^1 f(l)g(l)dl$.

II. OPTIMAL PROBLEM FORMULATION

In MHD flow, due to the non-physical interaction, one best feasible and efficient way of changing the fluid velocity or realizing a desired fluid velocity is through manipulation of the magnetic field. In this paper, our aim is to control the external magnetic input $\varrho(t)$ optimally so that the output flow velocity $u(l,t)$ can be brought as close as possible to the stationary state $u(l,T) = 0$ at the given time T. This manipulation is very crutial for many applications of the MHD flow systems with the purpose of enhance mixing or suppress turbulence. Thus, in this paper, we propose the following cost functional to be minimized:

$$J(u,\varrho(t)) = \frac{\lambda_1}{2}\int_0^1 u^2(l,T)dl + \frac{\lambda_2}{2}\int_0^T \varrho^2(t)dt, \qquad (3)$$

where $\lambda_1 \geq 0$ and $\lambda_2 \geq 0$ are non-negative weighting constants. The first term in (3) is to penalty the flow velocity $u(l,T)$ at the terminal time, and the second term in (3) is to penalty the energy of the magnetic input.

Recalling that the control input $\varrho(t)$ satisfies physical constraint (2), any valued piecewise-continuous function $\varrho(t)$ that satisfies the bound constraint (2) is called an admissible control. Let Θ be the class of all such admissible control. Now, we state our dynamic optimal control problem formally as follows.

Problem P_0: Given the PDE system (1) with the boundary conditions and initial condition, the aim is to find an admissible control $\varrho(t) \in \Theta$ such that the cost functional (3) is minimized.

III. SEMI-DISCRETE APPROXIMATION PROBLEM

In this section, the ROM technique will be used to approximate the original distributed optimal Problem P_0 as a semi-discrete approximation problem. We will first give a brief formulation of the POD basis functions computation, then combine the POD model reduction theory with Galerkin projection to reduce the original PDEs system into a low order dynamical system modeled by ODEs, and thus will lead to another more simple optimal control problem to be solved for the MHD flow system.

A. POD METHOD BASED ON SNAPSHOTS

Consider the following dynamical system modeled by a nonlinear PDEs form

$$\dot{z}(t,x) = \mathcal{F}(z(t,x), p, u(t)) \in \mathcal{Z}, \qquad (4)$$

where $\mathcal{Z}$ denotes an infinite-dimension Hilbert space, $z(t,x)$ denotes the states, $p \in \mathbb{R}^m$ denotes physical parameters in the dynamical system, $u(t)$ is the vector of control inputs. The basis idea of the POD method is to find a set of optimal spatial basis functions $\mathcal{V} = \{\upsilon_1(x), \upsilon_2(x), \ldots, \upsilon_l(x)\}$ $(l \leq s)$ that can capture most energy of the original PDEs from a given collection of snapshots over a finite time solutions of the PDEs $\mathcal{S}_z = \{z(t_1,x), z(t_2,x), \ldots, z(t_s,x)\} = \{z_i(x)\}, i = 1, 2 \ldots, s$. These snapshots can be obtained by solving an approximation of the high-dimensional PDEs or from the observed experimental data. Based on the optimal basis functions $\upsilon_i(x)$, the original PDE system can be then approximated as

$$z(t,x) \approx \Phi z^{pod}(t,x) = \sum_{i=1}^{l} q_i(t)\upsilon_i(x), \qquad (5)$$

where Φ is a $s \times r$ matrix containing the basis functions $\upsilon_i(x)$.

To obtain the optimal basis functions $\upsilon_i(x)$ by the snapshots method [34], the POD method is to minimize the following projection error of given data set $\mathcal{S}_z$ onto the subspace, i.e.,

$$\begin{aligned} &\min_{\upsilon_i(x)\in\mathcal{V}} J^{pod}(\upsilon_1, \upsilon_2, \ldots, \upsilon_l) \\ &\quad = \sum_{i=1}^{s}\Big\langle \sum_{j=1}^{l}\langle z_i, \upsilon_j\rangle\upsilon_j - \upsilon_i, \sum_{j=1}^{l}\langle z_i, \upsilon_j\rangle\upsilon_j - \upsilon_i\Big\rangle, \\ &\text{s.t. } \langle \upsilon_i, \upsilon_j\rangle = \delta_{ij} = \begin{cases} 1, & \text{if } i < j, \\ 0, & \text{if } i \neq j. \end{cases} \end{aligned} \qquad (6)$$

Problem (6) can be commonly solved by many existed optimization algorithms. According to the proof in [35], the i-th optimal POD basis function can be obtained by

$$\upsilon_i(x) = \frac{1}{\sqrt{\lambda_i^z}}\sum_{j=1}^{j=s}\xi_i^z(j)z(t_j,x), \quad i = 1, 2, \ldots, r_{pod}, \qquad (7)$$

where $r_{pod} \leq s$ is the number of retained POD basis functions and λ_i^z, $\xi_i^z(j)$ are elements of the normalized eigenvalues and eigenvectors of correlation matrix K^z whose elements are defined as

$$K_{ij}^z = \frac{1}{s} < z(t_i,x), z(t_j,x) >, \quad i,j = 1, 2, \ldots, s. \qquad (8)$$

By incorporating (5) and the POD basis functions $\upsilon_i(x)$ obtained in (7), then the original PDE system (4) can be projected on the reduced dimension POD space by using a Galerkin projection. This will lead to an ODE system in form

$$\dot{\boldsymbol{q}}^{pod}(t) = \boldsymbol{f}(\boldsymbol{q}^{pod}(t), p, u(t)) \in \mathbb{R}^{r_{pod}}, \qquad (9)$$

where $\boldsymbol{q}^{pod}(t)$ denotes the POD projection coefficients and $\boldsymbol{f}$ is related to the structure of the original PDE (4). In the following section, we will give the detailed procedure for the reduce-order model by using the Galerkin projection method.

B. REDUCED-ORDER MODEL VIA GALERKIN PROJECTION

Let υ_1 and υ_2 be trial functions, respectively. We now take the normal inner product of (1) with υ_1 and υ_2 to obtain the weak form of the original PDEs

$$\begin{cases} < \upsilon_1(l), u_t(l,t) > = < \upsilon_1(l), \nu u_{ll}(l,t) > \\ \quad + < \upsilon_1(l), \varrho(t) B_l(l,t) > - < \upsilon_1(l), p(t) >, & \text{(10a)} \\ < \upsilon_2(l), B_t(l,t) > = < \upsilon_2(l), \nu_m B_{ll}(l,t) > \\ \quad + < \upsilon_2(l), \varrho(t) u_l(l,t) > . & \text{(10b)} \end{cases}$$

Using integration by parts on the right-hand side of (10), we obtain

$$\begin{cases} < \upsilon_1(l), u_t(l,t) > = \nu\upsilon_1(1)u_l(1,t) - \nu\upsilon_1(0)u_l(0,t) > \\ - < \upsilon_1'(l), \nu u_l(l,t) > - < \upsilon_1'(l), \varrho(t) B(l,t) > \\ - < \upsilon_1(l), p(t) >, & \text{(11a)} \\ < \upsilon_2(l), B_t(l,t) > = \nu_m\upsilon_2(1)B_l(1,t) - \nu_m\upsilon_2(0)B_l(0,t) \\ - < \upsilon_2'(l), \nu_m B_l(l,t) > - < \upsilon_2'(l), u(l,t)\varrho(t) > . \\ & \text{(11b)} \end{cases}$$

Now, we assume the flow velocity $u(l,t)$ and the magnetic $B(l,t)$ in (1) can be spanned by the POD basis functions ϕ_i, ψ_i, i.e.,

$$u(l,t) \approx u^{pod}(l,t) = \sum_{i=1}^{r_1} u_i^{pod}(t)\phi_i(l), \quad \text{(12a)}$$

$$B(l,t) \approx B^{pod}(l,t) = \sum_{i=1}^{r_2} B_i^{pod}(t)\psi_i(l), \quad \text{(12b)}$$

where $u_i^{pod}(t), B_i^{pod}(t)$, $i = 1, \ldots, r_1$, are weighting functions to be determined.

By substituting (12a) into the weak form (11a) and choosing the trial function $\upsilon_1(l)$ as the POD basis functions $\phi_j(l), j = 1, \ldots, r_1$, we can obtain

$$\begin{aligned} &< \phi_j(l), \sum_{i=1}^{r_1} \dot{u}_i^{pod}(t)\phi_i(l) > \\ &= \nu\phi_j(1)\sum_{i=1}^{r_1} u_i^{pod}(t)\phi_i'(1) - \nu\phi_j(0)\sum_{i=1}^{r_1} u_i^{pod}(t)\phi_i'(0) \\ &\quad - < \phi_j'(l), \nu\sum_{i=1}^{r_1} u_i^{pod}(t)\phi_i'(l) > \\ &\quad - < \phi_j'(l), \varrho(t)\sum_{i=1}^{r_2} B_i^{pod}(t)\psi_i(l) > \\ &\quad - < \phi_j(l), p(t) > . \end{aligned} \quad \text{(13)}$$

Similarly, substituting (12b) into the weak form (11b) and choosing $\upsilon_2(l) = \psi_j(l), j = 1, \ldots, r_2$, we can obtain

$$\begin{aligned} &< \psi_j(l), \sum_{i=1}^{r_2} \dot{B}_i^{pod}(t)\psi_i(l) > \\ &= \nu_m\psi_j(1)\sum_{i=1}^{r_2} B_i^{pod}(t)\psi_i'(1) - \nu_m\psi_j(0)\sum_{i=1}^{r_2} B_i^{pod}(t)\psi_i'(0) \\ &\quad - < \psi_j'(l), \nu_m\sum_{i=1}^{r_2} B_i^{pod}(t)\psi_i'(l) > \\ &\quad - < \psi_j'(l), \varrho(t)\sum_{i=1}^{r_1} u_i^{pod}(t)\phi_i(l) > . \end{aligned} \quad \text{(14)}$$

Now, we introduce the following notations:

$$\begin{aligned} \boldsymbol{u}^{pod}(t) &= [u_1^{pod}(t), u_2^{pod}(t), \ldots, u_{r_1}^{pod}(t)]^\top, \\ \boldsymbol{B}^{pod}(t) &= [B_1^{pod}(t), B_2^{pod}(t), \ldots, B_{r_2}^{pod}(t)]^\top, \\ \boldsymbol{A} &= [< \phi_i(l), \phi_j(l) >] \in \mathbf{R}^{r_1\times r_1}, \\ \tilde{\boldsymbol{A}} &= [< \psi_i(l), \psi_j(l) >] \in \mathbf{R}^{r_2\times r_2}, \\ \boldsymbol{C} &= [< \phi_i'(l), \phi_j'(l) >] \in \mathbf{R}^{r_1\times r_1}, \\ \tilde{\boldsymbol{C}} &= [< \psi_i'(l), \psi_j'(l) >] \in \mathbf{R}^{r_2\times r_2}, \\ \boldsymbol{E} &= [< \phi_i'(l), \psi_j(l) >] \in \mathbf{R}^{r_1\times r_1}, \\ \tilde{\boldsymbol{E}} &= [< \phi_i'(l), \psi_j(l) >] \in \mathbf{R}^{r_2\times r_2}, \\ \boldsymbol{F} &= [\phi_i(1)\phi_j'(1)] \in \mathbf{R}^{r_1\times r_1}, \\ \tilde{\boldsymbol{F}} &= [\phi_i(0)\phi_j'(0)] \in \mathbf{R}^{r_1\times r_1}, \\ \boldsymbol{G} &= [\psi_i(1)\psi_j'(1)] \in \mathbf{R}^{r_2\times r_2}, \\ \tilde{\boldsymbol{G}} &= [\psi_i(0)\psi_j'(0)] \in \mathbf{R}^{r_2\times r_2}, \\ \boldsymbol{d} &= [< \phi_j(l), 1 >] \in \mathbf{R}^{r_1\times 1}, . \end{aligned}$$

Then, equations (13)-(14) can be rewritten in following matrix forms:

$$\begin{cases} \boldsymbol{A}\dot{\boldsymbol{u}}^{pod}(t) = (\boldsymbol{F} - \nu\tilde{\boldsymbol{F}} - \nu\boldsymbol{C})\boldsymbol{u}^{pod}(t) \\ \qquad\qquad -\varrho(t)\boldsymbol{E}\boldsymbol{B}^{pod}(t) - p(t)\boldsymbol{d}, & \text{(15a)} \\ \tilde{\boldsymbol{A}}\dot{\boldsymbol{B}}^{pod}(t) = (\boldsymbol{G} - \nu_m\tilde{\boldsymbol{G}} - \nu_m\tilde{\boldsymbol{C}})\boldsymbol{B}^{pod}(t) \\ \qquad\qquad -\varrho(t)\tilde{\boldsymbol{E}}\cdot\boldsymbol{u}^{pod}(t), & \text{(15b)} \end{cases}$$

To simplify the notations, let

$$\begin{aligned} \boldsymbol{x}(t) = \Big[&u_1^{pod}(t), u_2^{pod}(t), \ldots, u_{r_1}^{pod}(t), \\ &B_1^{pod}(t), B_2^{pod}(t), \ldots, B_{r_2}^{pod}(t)\Big]^\top \in \mathbb{R}^n, n = r_1 + r_2. \end{aligned}$$

Then, (15) can be written in the following compact form

$$\dot{\boldsymbol{x}}(t) = \hat{\boldsymbol{A}}^{-1}\left[\hat{\boldsymbol{C}}\boldsymbol{x}(t) - \varrho(t)\hat{\boldsymbol{E}}\boldsymbol{x}(t) - p(t)\hat{\boldsymbol{d}}\right], \quad \text{(16)}$$

where

$$\hat{\boldsymbol{A}} = \begin{bmatrix} \boldsymbol{A} & \boldsymbol{0} \\ \boldsymbol{0} & \tilde{\boldsymbol{A}} \end{bmatrix} \in \mathbb{R}^{n\times n},$$

$$\hat{\boldsymbol{C}} = \begin{bmatrix} \boldsymbol{F} - \nu\tilde{\boldsymbol{F}} - \nu\boldsymbol{C} & \boldsymbol{0} \\ \boldsymbol{0} & -\nu_m\boldsymbol{G} - \nu_m\tilde{\boldsymbol{G}} - \nu_m\tilde{\boldsymbol{C}} \end{bmatrix} \in \mathbb{R}^{n\times n},$$

$$\hat{\boldsymbol{d}} = \begin{bmatrix} \boldsymbol{d} & \boldsymbol{0} \end{bmatrix}^\top \in \mathbb{R}^n,$$

$$\hat{\boldsymbol{E}} = \begin{bmatrix} \boldsymbol{0} & \boldsymbol{E} \\ \tilde{\boldsymbol{E}} & \boldsymbol{0} \end{bmatrix} \in \mathbb{R}^{n\times n}.$$

For the initial conditions in (1), they can be written as

$$\begin{cases} u_0(l) = \sum_{i=1}^{r} u_i^{pod}(0)\phi_i(l), & \text{(17a)} \\ B_0(l) = \sum_{i=1}^{r} B_i^{pod}(0)\psi_i(l). & \text{(17b)} \end{cases}$$

Multiplying both sides of (17) by the POD basis functions $\phi_j(l)$, $\psi_j(l)$ and integrating over $l \in [0, 1]$, it obtains

$$\begin{cases} < \phi_j(l), u_0(l) > = < \phi_j(l), \sum_{i=1}^{r_1} u_i^{pod}(0)\phi_i(l) >, & (18a) \\ < \psi_j(l), B_0(l) > = < \psi_j(l), \sum_{i=1}^{r_2} B_i^{pod}(0)\psi_i(l) >, & (18b) \end{cases}$$

We introduce the following matrix notations

$$\begin{aligned} \tilde{g}_j &= < \phi_j(l), u_0(l) >, \quad j = 1, 2, \ldots, r_1, \\ \tilde{h}_j &= < \psi_j(l), B_0(l) >, \quad j = 1, 2, \ldots, r_2. \end{aligned} \tag{19}$$

Therefore, (18) can be also written in matrix forms as:

$$\boldsymbol{A}\boldsymbol{u}^{pod}(0) = \tilde{\boldsymbol{g}}, \quad \tilde{\boldsymbol{A}}\boldsymbol{B}^{pod}(0) = \tilde{\boldsymbol{h}}, \tag{20}$$

where $\tilde{\boldsymbol{g}} = [\tilde{g}_1, \tilde{g}_2, \ldots, \tilde{g}_{r_1}]^\top$, $\tilde{\boldsymbol{h}} = [\tilde{h}_1, \tilde{h}_2, \ldots, \tilde{h}_{r_2}]^\top$. Thus, we have

$$\begin{cases} \boldsymbol{u}^{pod}(0) = \boldsymbol{A}^{-1}\tilde{\boldsymbol{g}}, & (21a) \\ \boldsymbol{B}^{pod}(0) = \tilde{\boldsymbol{A}}^{-1}\tilde{\boldsymbol{h}}. & (21b) \end{cases}$$

As a result, the initial condition for dynamic system (16) can be defined as

$$\begin{aligned} \boldsymbol{x}(0) = \boldsymbol{x}_0 = \Big[& u_1^{pod}(0), u_2^{pod}(0), \ldots, u_{r_1}^{pod}(0), \\ & B_1^{pod}(0), B_2^{pod}(0), \ldots, B_{r_2}^{pod}(0) \Big]^\top \in \mathbb{R}^n. \end{aligned} \tag{22}$$

For the terminal state $u(l, T)$, based on the expansion (12a), it can be approximated as follows:

$$u^{pod}(l, T) = \sum_{i=1}^{r_1} u_i^{pod}(T)\phi_i(l), \tag{23}$$

where $u_i^{pod}(T), i = 1, 2, \ldots, r$, are weighting coefficients. Substituting (23) into the cost functional (3), we obtain

$$\begin{aligned} & J(\boldsymbol{x}(t), \varrho(t)) \\ &= \frac{\lambda_1}{2}\int_0^1 \left[\sum_{i=1}^{r_1} u_i^{pod}(T)\phi_i(l)\right]^2 dl + \frac{\lambda_2}{2}\int_0^T \varrho^2(t)dt \\ &= \frac{\lambda_1}{2}\sum_{i=1}^{r_1}\sum_{j=1}^{r_1} u_i^{pod}(T)\left[\int_0^1 \phi_i(l)\phi_j(l)dl\right] u_j^{pod}(T) \\ &\quad + \frac{\lambda_2}{2}\int_0^T \varrho^2(t)dt \\ &= \frac{\lambda_1}{2}\left[\boldsymbol{u}^{pod}(T)\right]^\top \boldsymbol{A}\left[\boldsymbol{u}^{pod}(T)\right] + \frac{\lambda_2}{2}\int_0^T \varrho^2(t)dt \\ &= \frac{\lambda_1}{2}\boldsymbol{x}_{1:r_1}^\top(T)\boldsymbol{A}\boldsymbol{x}_{1:r_1}(T) + \frac{\lambda_2}{2}\int_0^T \varrho^2(t)dt, \end{aligned} \tag{24}$$

where $\boldsymbol{x}_{1:r_1} = [u_1^{pod}(T), u_2^{pod}(T), \ldots, u_{r_1}^{pod}(T)]^\top$. Problem P_0, the distributed parameter optimal control problem, is now approximated by the following lumped parameter optimal control problem, which is defined as the following Problem P_1.

Problem P_1: Given the dynamic ODEs system (16) with the initial conditon (22), the aim is to find an admissiable control $\varrho(t) \in \Theta$ such that the cost function (24) is minimized.

IV. OPTIMAL CONTROL COMPUTATION

A. PIECEWISE-LINEAR CONTROL PARAMETERIZATION

Based on the POD method and Galerkin projection in previous section, Problem P_1 has become a semi-discrete optimal control problem governed by lumped parameter system. However, it is difficult, or impossible to provide the direct design of optimal control strategies for such problems. Thus, it is necessary to solve Problem P_1 numerically. Now we develop an efficient dynamic optimization method which is based on the control parameterization approach [36]–[38] to solve the approximation Problem P_1. The control parameterization method is a popular computational optimal control approach for solving nonlinear dynamic optimization problems [39]–[43], where the time horizon is subdivided into a number of subintervals and the control function is normally approximated by a piecewise-constant function with possible discontinuities at a set of pre-assigned switching points. Then, the heights of this piecewise-constant function are regarded as decision variables to be selected optimally. Each of them can be solved as a nonlinear programming problem by using a gradient-based strategy.

We use the piecewise-linear basis functions to approximate the control input $\varrho(t)$ instead of the conventional piecewise-constant control approximation because the induction of the external magnetic field $\varrho(t)$ in reality is required to be continuous. More specifically, we first subdivide the time horizon $[0, T]$ into p subintervals $[t_{k-1}, t_k)$, $k = 1, 2, \ldots, p$, where $t_k, k = 0, 1, \ldots, p$, are monotonically increasing sequences and $t_0 = 0$ and $t_p = T$, and the interior knot points $t_k, k = 1, 2, \ldots, p-1$, are predefined parameters, i.e.,

$$\tau_{\min} \le t_k - t_{k-1} \le \tau_{\max}, \quad k = 1, 2, \ldots, p. \tag{25}$$

Here, $\tau_{\min} > 0$ and $\tau_{\max} > 0$ are the minimum and maximum subinterval durations, respectively.

Then, we approximate the derivative of the control function $\varrho(t)$ on each time subinterval as follows:

$$\dot{\varrho}(t) \approx \sigma_k, \quad t \in [t_{k-1}, t_k), \ k = 1, 2, \ldots, p, \tag{26}$$

Here, σ_k denotes the approximation of the derivative of $\varrho(t)$ on each subinterval $[t_{k-1}, t_k)$. Mathematically, we can express (26) as follows:

$$\dot{\varrho}(t) \approx \dot{\varrho}^p(t) = \sum_{k=1}^{p} \sigma_k \chi_{[t_{k-1}, t_k)}(t), \quad t \in [0, T], \tag{27}$$

where $\chi_{[t_{k-1}, t_k)} : \mathbb{R} \to \mathbb{R}$ is the indicator function defined by

$$\chi_{[t_{k-1}, t_k)}(t) = \begin{cases} 1, & \text{if } t \in [t_{k-1}, t_k), \\ 0, & \text{otherwise.} \end{cases} \tag{28}$$

Based on (27), we can know the control function $\varrho(t)$ is piecewise-linear with jumps in the derivative at each time points $t_1, t_2, \ldots, t_{p-1}$. Now we introduce another new state variables $x_{n+1}(t)$ governed by the following state dynamics:

$$\begin{cases} \dot{x}_{n+1}(t) = \sum_{k=1}^{p} \sigma_k \chi_{[t_{k-1}, t_k)}(t), \quad t \in [0, T], & (29a) \\ x_{n+1}(0) = x_{n+1}^0. & (29b) \end{cases}$$

Then, the dynamic system (16) becomes

$$\begin{aligned}\dot{\boldsymbol{x}}(t) &= \boldsymbol{f}(t, \boldsymbol{x}(t), x_{n+1}(t)) \\ &= \hat{\boldsymbol{A}}^{-1}\left[\hat{\boldsymbol{C}}\boldsymbol{x}(t) - x_{n+1}(t)\hat{\boldsymbol{E}}\boldsymbol{x}(t) - p(t)\hat{\boldsymbol{d}}\right], \end{aligned} \tag{30}$$

We denote $\boldsymbol{\sigma} = [\sigma_1, \sigma_2, \ldots, \sigma_p]^\top \in \mathbb{R}^p$ and let $\boldsymbol{x}^p(\cdot|\boldsymbol{\sigma})$, $x^p_{n+1}(\cdot|\boldsymbol{\sigma})$ denote the solutions of system (30) and (29) corresponding to $\boldsymbol{\sigma}$, respectively. To determine $\boldsymbol{x}^p(\cdot|\boldsymbol{\sigma})$ and $x^p_{n+1}(\cdot|\boldsymbol{\sigma})$, we can solve (29)-(30) sequentially over the subintervals $[t_{k-1}, t_k)$, $k = 1, 2, \ldots, p$.

Recall that the control function $\varrho(t)$ in system (1) must be satisfied the physical constraint (2). Thus, the following continuous state inequality constraint on the new state variables x_{N+1} is now satisfied

$$0 \le x^p_{N+1}(t|\boldsymbol{\sigma}) \le \varrho_{max}, \quad t \in [0, T]. \tag{31}$$

Clearly, since $x_{N+1}(t)$ is piecewise-linear with break points at $t = t_1, t_2, \ldots, t_{p-1}$, the continuous state inequality constraint (31) is also equivalent to the following constraint:

$$0 \le x^p_{N+1}(t_k|\boldsymbol{\sigma}) \le \varrho_{max}, \quad k = 0, 1, \ldots, p. \tag{32}$$

Such constraints are special cases of the well-known canonical form in the optimal control literatures (see [37]).

Now, under the approximation (27), the cost functional (24) becomes

$$\begin{aligned}\mathcal{J}^p(\boldsymbol{x}(t), \boldsymbol{\sigma}) = \frac{\lambda_1}{2}[\boldsymbol{x}^p_{1:r_1}(T|\boldsymbol{\sigma})]^\top \boldsymbol{A}[\boldsymbol{x}^p_{1:r_1}(T|\boldsymbol{\sigma})] \\ + \frac{\lambda_2}{2}\sum_{k=1}^{p}\int_{t_{k-1}}^{t_k} x^p_{n+1}(t|\boldsymbol{\sigma})^2 dt. \end{aligned} \tag{33}$$

Now we state the new approximate optimal control problem as follows.

Problem P_2: Given the lumped parameter system (29)-(30), the objective is now to find a control parameter vector $\boldsymbol{\sigma}$ such that the cost functional (33) is minimized subject to constraint (32).

B. GRADIENT COMPUTATION

Actually, Problem P_2 is now become an optimal parameter selection problem in canonical form [36], which can be solved as a typical nonlinear optimization problem by using the SQP method based on the gradients of the cost function. We now show that these gradients can be obtained by the following lemma.

Lemma 1: The gradients of cost function (33) with respect to σ_k, $k = 1, 2, \ldots, p$ are given as

$$\begin{aligned}\frac{\partial \tilde{J}^p(\boldsymbol{x}(t), \boldsymbol{\sigma})}{\partial \sigma_k} = \frac{\lambda_1}{2}[\boldsymbol{x}^p_{1:r_1}(T|\boldsymbol{\sigma})]^\top \boldsymbol{A}\boldsymbol{\varphi}^k_{1:r_1}(T|\boldsymbol{\sigma}) \\ + \lambda_2 \sum_{k=1}^{p}\int_{t_{k-1}}^{t_k} x^p_{n+1}(t|\boldsymbol{\sigma})\frac{\partial x^p_{n+1}(t|\boldsymbol{\sigma})}{\partial \sigma_k} dt. \end{aligned} \tag{34}$$

where $\boldsymbol{\varphi}^k_{1:r_1}(\cdot|\boldsymbol{\sigma})$ denotes the first r_1 solutions of (35) corresponding to $\boldsymbol{\sigma}$, and the state variations $\boldsymbol{\varphi}_k(t|\boldsymbol{\sigma}) = \frac{\partial \boldsymbol{x}^p(t|\boldsymbol{\sigma})}{\partial \sigma_k}$ are satisfied:

$$\begin{cases} \dot{\boldsymbol{\varphi}}_k(t) = \dfrac{\partial \boldsymbol{f}(t, \boldsymbol{x}(t|\boldsymbol{\sigma}), x_{n+1}(t|\boldsymbol{\sigma}))}{\partial \boldsymbol{x}}\boldsymbol{\varphi}_k(t) \\ \qquad + \dfrac{\partial \boldsymbol{f}(t, \boldsymbol{x}(t|\boldsymbol{\sigma}), x_{n+1}(t|\boldsymbol{\sigma}))}{\partial x_{n+1}}\dfrac{\partial x^p_{n+1}(t|\boldsymbol{\sigma})}{\partial \sigma_k}, \\ \qquad t \in [t_{l-1}, t_l), l = k, k+1, \ldots, p, \qquad (35a) \\ \boldsymbol{\varphi}_k(t) = \boldsymbol{0}, \quad t \le t_k. \qquad (35b) \end{cases}$$

Proof: For each $l = 1, 2, \ldots, p$, we can obtain (36) from (30)

$$\begin{aligned}\boldsymbol{x}^p(t|\boldsymbol{\sigma}) = \boldsymbol{x}^p(t_{l-1}|\boldsymbol{\sigma}) + \int_{t_{l-1}}^{t} \boldsymbol{f}(\eta, \boldsymbol{x}(\eta|\boldsymbol{\sigma}), x_{n+1}(\eta|\boldsymbol{\sigma}))d\eta, \\ t \in [t_{l-1}, t_l). \end{aligned} \tag{36}$$

If $k \le l$, then differentiating (36) with respect to σ_k gets

$$\begin{aligned}\frac{\partial \boldsymbol{x}^p(t|\boldsymbol{\sigma})}{\partial \sigma_k} = \frac{\partial \boldsymbol{x}^p(t_{l-1}|\boldsymbol{\sigma})}{\partial \sigma_k} \\ + \int_{t_{l-1}}^{t}\left\{\frac{\partial \boldsymbol{f}(\eta, \boldsymbol{x}(\eta|\boldsymbol{\sigma}), x_{n+1}(\eta|\boldsymbol{\sigma}))}{\partial \boldsymbol{x}}\frac{\partial \boldsymbol{x}(\eta|\boldsymbol{\sigma})}{\partial \sigma_k}\right\}d\eta, \\ + \int_{t_{l-1}}^{t}\left\{\frac{\partial \boldsymbol{f}(\eta, \boldsymbol{x}(\eta|\boldsymbol{\sigma}), x_{n+1}(\eta|\boldsymbol{\sigma}))}{\partial x_{n+1}}\frac{\partial x^p_{n+1}(\eta|\boldsymbol{\sigma})}{\partial \sigma_k}\right\}d\eta, \\ t \in [t_{l-1}, t_l). \end{aligned} \tag{37}$$

If $k > l$, we have

$$\frac{\partial \boldsymbol{x}^p(t|\boldsymbol{\sigma})}{\partial \sigma_k} = \boldsymbol{0}, \quad t \in [t_{l-1}, t_l). \tag{38}$$

By differentiating (37) with respect to t, we obtain

$$\begin{aligned}\frac{d}{dt}\left\{\frac{\partial \boldsymbol{x}^p(t|\boldsymbol{\sigma})}{\partial \sigma_k}\right\} \\ = \left\{\frac{\partial \boldsymbol{f}(\eta, \boldsymbol{x}(\eta|\boldsymbol{\sigma}), x_{n+1}(\eta|\boldsymbol{\sigma}))}{\partial \boldsymbol{x}}\frac{\partial \boldsymbol{x}(\eta|\boldsymbol{\sigma})}{\partial \sigma_k}\right\}, \\ + \left\{\frac{\partial \boldsymbol{f}(\eta, \boldsymbol{x}(\eta|\boldsymbol{\sigma}), x_{n+1}(\eta|\boldsymbol{\sigma}))}{\partial x_{n+1}}\frac{\partial x^p_{n+1}(\eta|\boldsymbol{\sigma})}{\partial \sigma_k}\right\}, \\ t \in [t_{l-1}, t_l). \end{aligned} \tag{39}$$

For the initial condition (22), we have

$$\frac{\partial \boldsymbol{x}^p(0|\boldsymbol{\sigma})}{\partial \sigma_k} = \frac{\partial \boldsymbol{x}_0}{\partial \sigma_k} = \boldsymbol{0}. \tag{40}$$

It follows from (39)-(40) that, for each $k = 1, 2, \ldots, p$, the state variations $\boldsymbol{\varphi}_k(t|\boldsymbol{\sigma}) = \frac{\partial \boldsymbol{x}^p(t|\boldsymbol{\sigma})}{\partial \sigma_k}$ satisfy:

$$\begin{aligned}\dot{\boldsymbol{\varphi}}_k(t) = \frac{\partial \boldsymbol{f}(t, \boldsymbol{x}(t|\boldsymbol{\sigma}), x_{n+1}(t|\boldsymbol{\sigma}))}{\partial \boldsymbol{x}}\boldsymbol{\varphi}_k(t) \\ + \frac{\partial \boldsymbol{f}(t, \boldsymbol{x}(t|\boldsymbol{\sigma}), x_{n+1}(t|\boldsymbol{\sigma}))}{\partial x_{n+1}}\frac{\partial x^p_{n+1}(t|\boldsymbol{\sigma})}{\partial \sigma_k}, \\ t \in [t_{l-1}, t_l), l = k, k+1, \ldots, p, \end{aligned}$$

with the initial condition

$$\boldsymbol{\varphi}_k(t) = \boldsymbol{0}, \quad t \le t_k.$$

Therefore, the gradients $\frac{\partial \tilde{J}^p(\boldsymbol{x}(t), \boldsymbol{\sigma})}{\partial \sigma_k}$ can be obtained, as given in Lemma 1. □

Lemma 2: For each $l = 1, \ldots, p$, the state variation $\frac{\partial x^p_{n+1}(t|\boldsymbol{\sigma})}{\partial \sigma_k}$ on the interval $[t_{l-1}, t_l]$ is given by

$$\frac{\partial \tilde{x}^p_{N+1}(t|\boldsymbol{\sigma})}{\partial \sigma_k} = \begin{cases} t - t_{l-1}, & \text{if } k = l, \\ t_l - t_{l-1}, & \text{if } k < l, \\ 0, & \text{if } k > l. \end{cases} \tag{41}$$

Proof: For $l = 1$, it obtains from (29) that

$$\tilde{x}^p_{N+1}(t|\boldsymbol{\sigma}) = x^0_{N+1} + \sigma_1(t - t_0) = x^0_{N+1} + \sigma_1\, t, \quad t \in [0, t_1].$$

Clearly, for all $t \in [0, t_1]$, it satisfies

$$\frac{\partial x^p_{N+1}(t|\boldsymbol{\sigma})}{\partial \sigma_k} = \begin{cases} t, & \text{if } k = 1, \\ 0, & \text{if } k > 1, \end{cases}$$

which shows that (41) is satisfied for $l = 1$. Now, we suppose that (41) also holds for $l = q$. Then for all $s \in [t_{q-1}, t_q]$, it follows

$$\frac{\partial \tilde{x}^p_{N+1}(t|\boldsymbol{\sigma})}{\partial \sigma_k} = \begin{cases} t - t_{q-1}, & \text{if } k = q, \\ t_k - t_{k-1}, & \text{if } k < q, \\ 0, & \text{if } k > q. \end{cases}$$

For $l = q + 1$, we have from (29),

$$\tilde{x}^p_{N+1}(t|\boldsymbol{\sigma}) = \tilde{x}^p_{N+1}(t_q|\boldsymbol{\sigma}) + \sigma_{q+1}(t - t_q), \quad t \in [t_q, t_{q+1}].$$

Hence, for all $t \in [t_q, t_{q+1}]$,

$$\frac{\partial \tilde{x}^p_{N+1}(t|\boldsymbol{\sigma})}{\partial \sigma_k} = \begin{cases} t - t_q, & \text{if } k = q+1, \\ \frac{\partial \tilde{x}^p_{N+1}(t_q|\boldsymbol{\sigma})}{\partial \sigma_k}, & \text{if } k < q+1, \\ 0, & \text{if } k > q+1. \end{cases}$$

By the inductive hypothesis, we obtain

$$\frac{\partial \tilde{x}^p_{N+1}(t|\boldsymbol{\sigma})}{\partial \sigma_k} = \begin{cases} t - t_q, & \text{if } k = q+1, \\ t_k - t_{k-1}, & \text{if } k < q+1, \\ 0, & \text{if } k > q+1. \end{cases}$$

The above results show that (41) also hold for $l = q + 1$. Thus, we get Lemma 2. □

By incorporating Lemma 1 and Lemma 2 into a nonlinear programming algorithm such as SQP, then we can solve Problem P_2 numerically.

V. NUMERICAL ILLUSTRATES

In this section, we illustrate the numerical simulation example of the MHD flow system (1). The parameters are set $Re = 100$, $Re_m = 100$, $f(t) = 0.001$, and the initial conditions are chosen $u_0(l) = (2l^2 + 5)\sin(2\pi l)$, $B_0(l) = l^2 \sin(\pi l)$. All the snapshots that can generate the POD modes are obtained by solving an approximation of the original PDE system (1), e.g., using FEM method. Our codes also implement the gradient-based optimization procedure proposed in Section IV combined with the intrinsic subroutines algorithm SQP (e.g., performing the optimization steps).

A. POD MODES COMPUTATION

In order to compute the POD basis functions mathematically, we first need to get a collection of snapshots from the original PDEs (1). The approximation numerical solutions can be done by discretizing the original PDEs using any finite element basis functions such as piecewise-linear functions or cubic functions based on FEM method. We denote the approximation solutions of the system (1) by $u_{fem}(t, l)$ and $B_{fem}(t, l)$. Then, we choose a set of s snapshots from the solutions $\{u_{fem}(t, l), B_{fem}(t, l)\}$, i.e.,

$$\begin{aligned} \mathcal{S}_u &= \{u_{fem}(t_1, l), u_{fem}(t_2, l), \ldots, u_{fem}(t_s, l)\} \in \mathbb{R}^n, \\ \mathcal{S}_B &= \{B_{fem}(t_1, l), B_{fem}(t_2, l), \ldots, B_{fem}(t_s, l)\} \in \mathbb{R}^n. \end{aligned} \tag{42}$$

where n denotes the selected number of subintervals in the spatial domain by FEM basis element functions.

Next, we define the following correlation matrices elements of $\mathcal{S}_u$ and $\mathcal{S}_B$ as

$$K^u_{ij} = \frac{1}{s} < u_{fem}(t_i, l), u_{fem}(t_j, l) >, \quad i, j = 1, 2, \ldots, s, \tag{43a}$$

$$K^B_{ij} = \frac{1}{s} < B_{fem}(t_i, l), B_{fem}(t_j, l) >, \quad i, j = 1, 2, \ldots, s. \tag{43b}$$

Based on the correlation matrices (43) and (7), the optimal POD modes $\phi_i(l)$ and $\psi_i(l)$ can be computed throught the snapshots in (42). Let $\lambda^u_1 > \lambda^u_2 > \cdots > \lambda^u_l > \cdots > \lambda^u_{d_1} > 0$ and $\lambda^B_1 > \lambda^B_2 > \cdots > \lambda^B_l > \cdots > \lambda^B_{d_2} > 0$ denote the positive decreasing eigenvalues corresponding to the correlation matrices $\boldsymbol{K}^u$ and $\boldsymbol{K}^B$, respectively, where $d_1 = \text{rank}(\boldsymbol{K}^u)$ and $d_2 = \text{rank}(\boldsymbol{K}^B)$. The error energy ratios associated with the approximation with the first l POD modes can be approximation as [34]

$$\begin{aligned} \varepsilon^u_l &= \sum_{i=1}^{s} \Big\langle \sum_{j=1}^{l} \langle u_i, \phi_j \rangle \phi_j - \phi_i, \sum_{j=1}^{l} \langle u_i, \phi_j \rangle \phi_j - \phi_i \Big\rangle \\ &= \sum_{k=l+1}^{d_1} \lambda^u_k, \end{aligned} \tag{44a}$$

$$\begin{aligned} \varepsilon^B_l &= \sum_{i=1}^{s} \Big\langle \sum_{j=1}^{l} \langle B_i, \psi_j \rangle \psi_j - \psi_i, \sum_{j=1}^{l} \langle B_i, \psi_j \rangle \psi_j - \psi_i \Big\rangle \\ &= \sum_{k=l+1}^{d_2} \lambda^B_k \end{aligned} \tag{44b}$$

In this case, we can compute the energy of the original PDE system captured by the POD method from the simulated data, as shown in Fig. 2. We note that just three ($r_1 = 3$) POD modes are enough to capture more than 99% of the original system energy $u(l, t)$ and just four ($r_2 = 4$) POD modes for the original system energy $B(l, t)$. In Fig. 3, we show the first three POD basis functions $\phi_i, i = 1, 2, 3$ for $u(l, t)$ and the first four POD basis functions $\psi_i, i = 1, 2, 3, 4$ for $B(l, t)$. In Fig. 4, we also give a comparison of the corresponding system states $u(l, t)$ generated by FEM method and

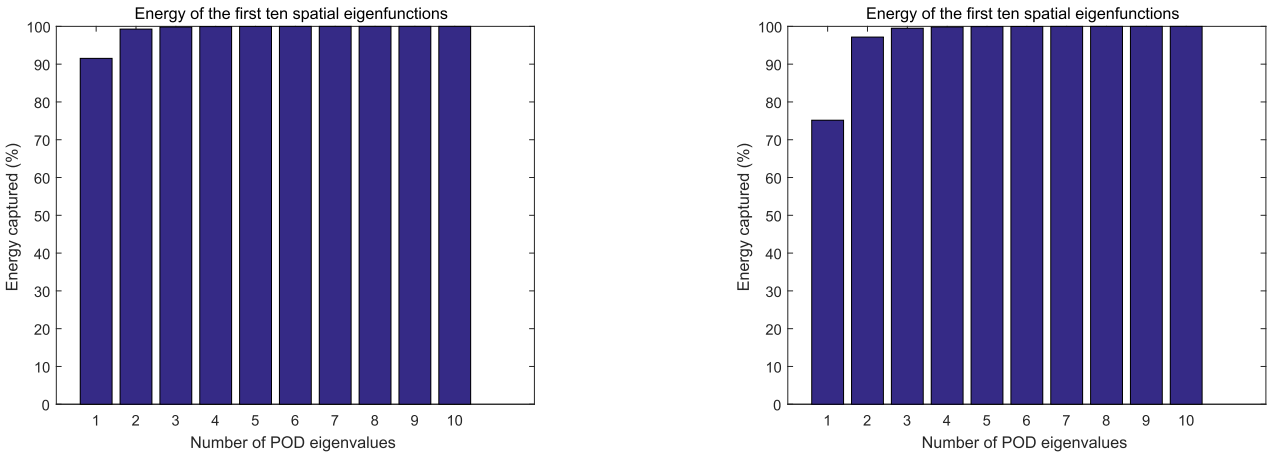

FIGURE 2. Energy of the first ten POD eigenvalues corresponding to snapshots of $u(l,t)$ and $B(l,t)$. (a) Energy of the first ten POD eigenvalues corresponding to snapshots of $u(l,t)$. (b) Energy of the first ten POD eigenvalues corresponding to snapshots of $B(l,t)$.

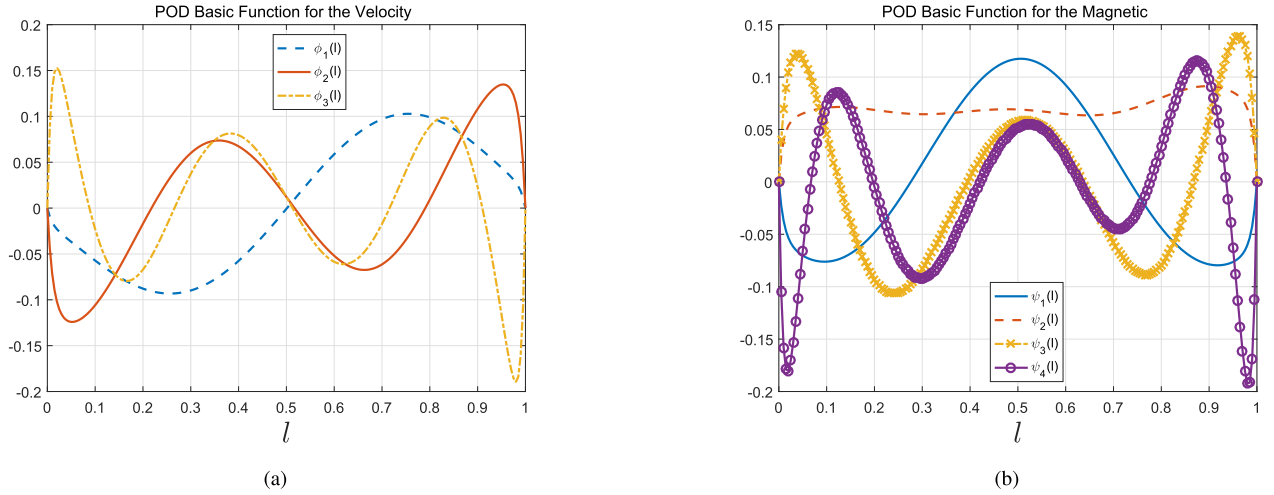

FIGURE 3. POD basis functions. (a) POD basis functions $\phi_i(l)$. (b) POD basis functions $\psi_i(l)$.

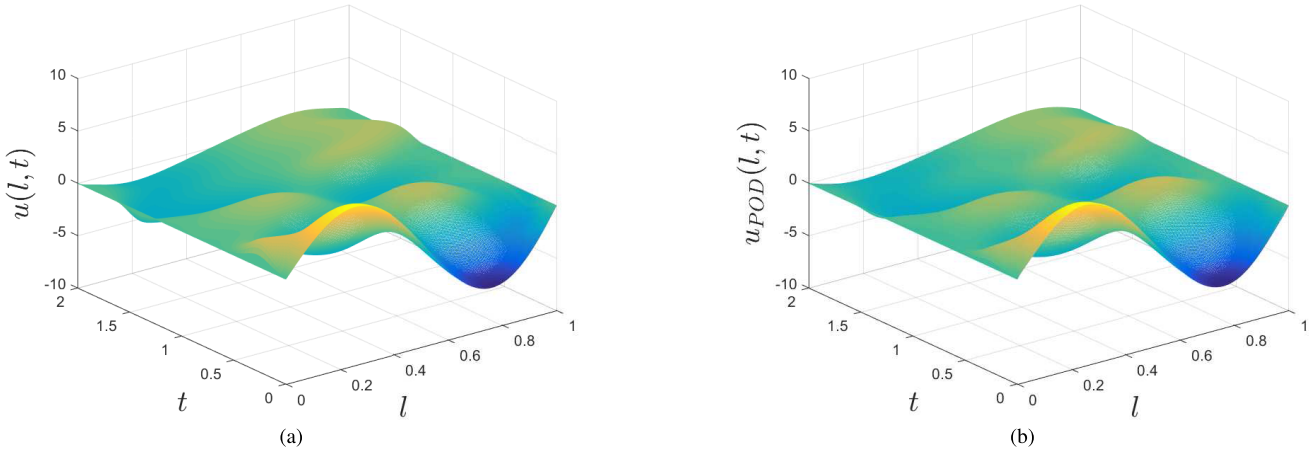

FIGURE 4. Flow velocity state $u(l,t)$ corresponding to the experimental input data. (a) Original state $u(l,t)$. (b) POD model $u(l,t)$.

POD model order reduction method. The numerical results validate again that the model reduction method using POD proposed in Section III is effective. Based on the MOR model, in next section, we will realize the optimal control problem by using the gradient-based method proposed in Section IV.

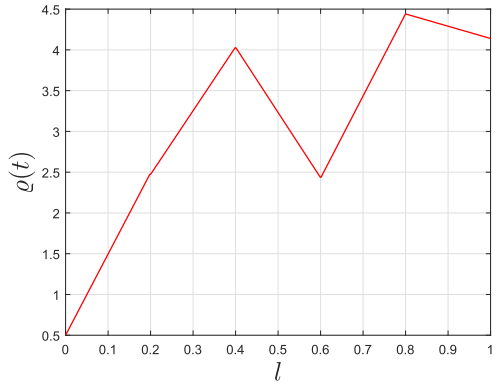

FIGURE 5. Optimal control input $\varrho(t)$ ($p = 5$).

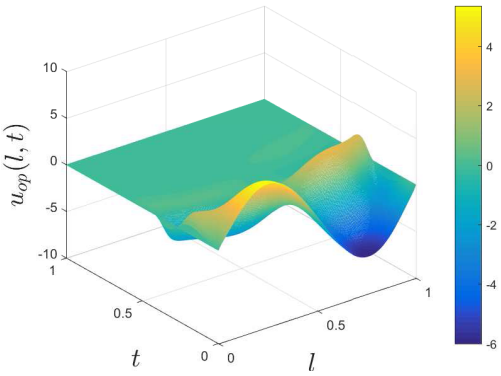

FIGURE 6. Optimal flow velocity $u(l;t)$($p = 5$).

B. COMPUTATION OF THE OPTIMAL CONTROLLER

Based on the piecewise-linear control parameterization technique proposed in Section IV, we first subdivide the time interval $[0, T] = [0, 1]$ into p subintervals. Then the control input function $\varrho(t)$ is parameterized as in form (27), in which t_k, $k = 1, 2, \ldots, p$, are equidistant switching time points in the interval $[0, 2]$, with $t_0 = 0$ and $t_p = 1$. Note that the approximate control in (27) switches value at the instants $t = t_k, k = 1, 2, \ldots, p-1$. The upper bound in (2) is given by $\beta_{\max} = 5$. Our MATLAB code implements the gradient-based optimization procedure by combining *fmincon* with the sensitivity method for gradient computation. We also use MATLAB's non-stiff differential equation solver ODE45 to integrate the state system and the sensitivity systems.

We first choose $p = 5$ for the subintervals. After the gradient-based optimization procedure terminated, we obtain the optimal piecewise-linear control input $\varrho(t)$, as shown in Fig. 5. The output flow velocity state $u(l, t)$ corresponding to the optimal control $\varrho(t)$ is shown in Fig. 6. The results show that our numerical optimization procedure can drive the final flow velocity $u(l, T)$ to 0 as the optimized control variables changing with time. This means that the flow velocity $u(x, t)$ can converge to stationary state under our designed optimal control input $\varrho(t)$ as the time evolution. The results clearly demonstrate that the control parameterization method combined with the POD model reduction method is effective at determining the optimal controls for the MHD flow velocity.

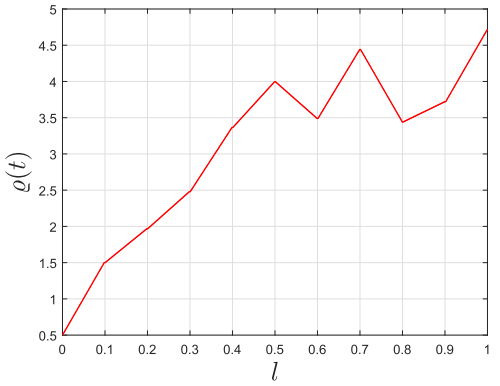

FIGURE 7. Optimal control input $\varrho(t)$ ($p = 10$).

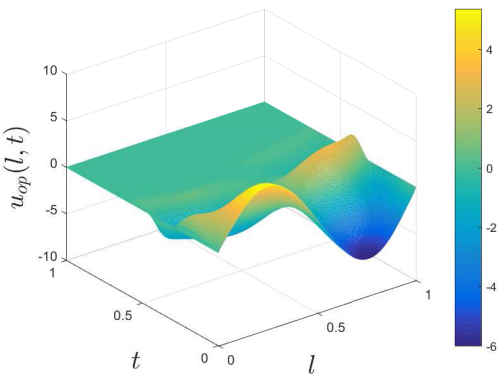

FIGURE 8. Optimal flow velocity $u(l, t)$ ($p = 10$).

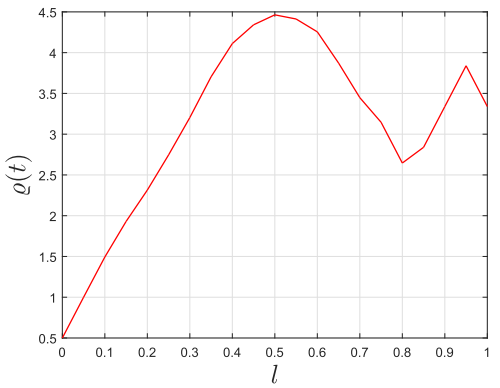

FIGURE 9. Optimal control input $\varrho(t)$ ($p = 20$).

We next increase the subinterval $p = 5$ to $p = 10$ for the time subintervals. The results of optimal control input $\varrho(t)$ and optimal output flow velocity state $u(l, t)$ are given in Figs. 7-8, respectively. Compared with the results with $p = 5$, the final output flow velocity is closer to the desired flow velocity target, as expected. We also increase $p = 10$ to $p = 20$ for the numerical simulations, as shown in Figs. 9-10. The results further verify the effectiveness of our proposed method. However, in our simulation procedure, we note that increasing p further does not result in any significant change in the objective functional value, despite an increase in the

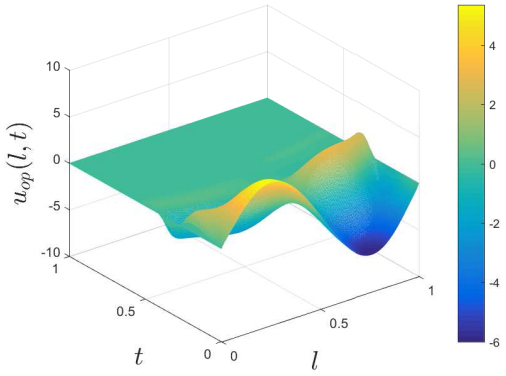

FIGURE 10. Optimal flow velocity $u(l,t)$ ($p = 20$).

overall computation time. Thus, choosing $p = 20$ is enough to obtain the optimal solutions.

VI. CONCLUSION

In this paper, we realize the optimal control of flow velocity arising in a novel 1-D MHD flow system with bilinear control actuation. A finite-time PDE-constrained optimal control problem is formulated and then solved successfully by using POD reduction technique and control parameterization method. Simulation results show that the gradient-based optimization procedure is efficient and can reduce the computational burden. The methodology proposed in this paper is also potential for the real-time implementation in a close-loop receding horizon scheme for the MHD flow systems.

REFERENCES

[1] D. Huang, J.-X. Xu, X. Li, C. Xu, and M. Yu, "D-type anticipatory iterative learning control for a class of inhomogeneous heat equations," *Automatica*, vol. 49, no. 8, pp. 2397–2408, 2013.

[2] Z. Zhen, S.-X. Tang, and Z. Zhou, "Stabilization of a heat-ODE system cascaded at a boundary point and an intermediate point," *Asian J. Control*, vol. 19, no. 5, pp. 1834–1843, 2017.

[3] S. Zhang, "Sliding mode control for an inhomogeneous heat equation with global constraint," *Asian J. Control*, vol. 19, no. 6, pp. 2116–2126, 2017.

[4] C. Xu, E. Schuster, R. Vazquez, and M. Krstic, "Stabilization of linearized 2D magnetohydrodynamic channel flow by backstepping boundary control," *Syst. Control Lett.*, vol. 57, no. 10, pp. 805–812, 2008.

[5] E. Schuster, L. Luo, and M. Krstić, "MHD channel flow control in 2D: Mixing enhancement by boundary feedback," *Automatica*, vol. 44, no. 10, pp. 2498–2507, 2008.

[6] W. He, S. Zhang, and S. S. Ge, "Robust adaptive control of a thruster assisted position mooring system," *Automatica*, vol. 50, no. 7, pp. 1843–1851, 2014.

[7] W. He, Y. Dong, and C. Sun, "Adaptive neural impedance control of a robotic manipulator with input saturation," *IEEE Trans. Syst., Man, Cybern., Syst.*, vol. 46, no. 3, pp. 334–344, Mar. 2016.

[8] W. He and S. Zhang, "Control design for nonlinear flexible wings of a robotic aircraft," *IEEE Trans. Control Syst. Technol.*, vol. 25, no. 1, pp. 351–357, Jan. 2017.

[9] Z. Liu, J. Liu, and W. He, "Partial differential equation boundary control of a flexible manipulator with input saturation," *Int. J. Syst. Sci.*, vol. 48, no. 1, pp. 53–62, 2017.

[10] Z. Liu and J. Liu, "Boundary control of a flexible robotic manipulator with output constraints," *Asian J. Control*, vol. 19, no. 1, pp. 332–345, 2017.

[11] H. Yang and Z. Liu, "Active control of an elastic beam based on state and input constraints," *IEEE Access*, vol. 46, pp. 10635–10643, 2018.

[12] Y. Ou *et al.*, "Optimal tracking control of current profile in tokamaks," *IEEE Trans. Control Syst. Technol.*, vol. 19, no. 2, pp. 432–441, Mar. 2011.

[13] C. Xu *et al.*, "Ramp-up-phase current-profile control of tokamak plasmas via nonlinear programming," *IEEE Trans. Plasma Sci.*, vol. 38, no. 2, pp. 163–173, Feb. 2010.

[14] C. Xu, Y. Ou, and E. Schuster, "Sequential linear quadratic control of bilinear parabolic PDEs based on POD model reduction," *Automatica*, vol. 47, no. 2, pp. 418–426, 2011.

[15] P. A. Davidson, *An Introduction to Magnetohydrodynamics*. Cambridge, U.K.: Cambridge Univ. Press, 2001.

[16] U. Müller and L. Bühler, *Magnetofluiddynamics in Channels and Containers*. Berlin, Germany: Springer, 2013.

[17] J. P. Goedbloed and S. Poedts, *Principles of Magnetohydrodynamics: With Applications to Laboratory and Astrophysical Plasmas*. Cambridge, U.K.: Cambridge Univ. Press, 2004.

[18] S. Qian and H. H. Bau, "Magneto-hydrodynamics based microfluidics," *Mech. Res. Commun.*, vol. 36, no. 1, pp. 10–21, 2009.

[19] I. Munteanu, "Boundary feedback stabilization of periodic fluid flows in a magnetohydrodynamic channel," *IEEE Trans. Autom. Control*, vol. 58, no. 8, pp. 2119–2125, Aug. 2013.

[20] Z. Ren, S. Guo, Z. Li, and Z. Wu, "Adjoint-based parameter and state estimation in 1-D magnetohydrodynamic (MHD) flow system," *J. Ind. Manage. Optim.*, vol. 15, pp. 1213–1218, Jan. 2018.

[21] L. D. Landau, L. Pitaevskii, and E. M. Lifshitz, *Electrodynamics of Continuous Media*. Amsterdam, The Netherlands: Elsevier, 2013.

[22] R. Vazquez and M. Krstic, *Control of Turbulent and Magnetohydrodynamic Channel Flows: Boundary Stabilization and State Estimation*. Boston, MA, USA: Springer, 2008.

[23] R. Vazquez, E. Schuster, and M. Krstic, "A closed-form full-state feedback controller for stabilization of 3D magnetohydrodynamic channel flow," *J. Dyn. Syst., Meas., Control*, vol. 131, no. 4, p. 041001, 2009.

[24] J. Baker and P. D. Christofides, "Drag reduction in transitional linearized channel flow using distributed control," *Int. J. Control*, vol. 75, no. 15, pp. 1213–1218, 2002.

[25] K. Debbagh, P. Cathalifaud, and C. Airiau, "Optimal and robust control of small disturbances in a channel flow with a normal magnetic field," *Phys. Fluids*, vol. 19, no. 1, p. 014103, 2007.

[26] J.-L. Wang, H.-N. Wu, T. Huang, S.-Y. Ren, and J. Wu, "Pinning control for synchronization of coupled reaction-diffusion neural networks with directed topologies," *IEEE Trans. Syst., Man, Cybern., Syst.*, vol. 46, no. 8, pp. 1109–1120, Aug. 2016.

[27] C. Xu, Y. Dong, Z. Ren, H. Jiang, and X. Yu, "Sensor deployment for pipeline leakage detection via optimal boundary control strategies," *J. Ind. Manage. Optim.*, vol. 11, no. 1, pp. 199–216, 2015.

[28] W. He and S. S. Ge, "Vibration control of a flexible string with both boundary input and output constraints," *IEEE Trans. Control Syst. Technol.*, vol. 23, no. 4, pp. 1245–1254, Jul. 2015.

[29] J. L. Wang, H. N. Wu, T. W. Huang, and R. S. Yan, "Pinning control strategies for synchronization of linearly coupled neural networks with reaction–diffusion terms," *IEEE Trans. Neural Netw. Learn. Syst.*, vol. 27, no. 4, pp. 749–761, Jun. 2016.

[30] Z. J. Zhao, Y. Liu, and F. Luo, "Boundary control for a vibrating string system with bounded input" *Asian J. Control*, vol. 20, no. 1, pp. 323–331, 2018.

[31] C. Xu and E. Schuster, "Low-dimensional modeling of linear heat transfer systems using incremental the proper orthogonal decomposition method," *Asia–Pacific J. Chem. Eng.*, vol. 8, no. 4, pp. 473–482, 2013.

[32] K. Li, H. Su, J. Chu, and C. Xu, "A fast-POD model for simulation and control of indoor thermal environment of buildings," *Building Environ.*, vol. 60, pp. 150–157, Feb. 2013.

[33] P. Benner, E. Sachs, and S. Volkwein, *Model Order Reduction for PDE Constrained Optimization*. Basel, Switzerland: Springer International Publishing, 2014.

[34] W. H. Schilders, H. A. Van der Vorst, and J. Rommes, *Model Order Reduction: Theory, Research Aspects and Applications*, vol. 13. Berlin, Germany: Springer, 2008.

[35] K. Kunisch and S. Volkwein, "Galerkin Proper orthogonal decomposition methods for a general equation in fluid dynamics," *SIAM J. Numer. Anal.*, vol. 40, no. 2, pp. 492–515, 2002.

[36] K. L. Teo, C. J. Goh, and K. H. Wong, *A Unified Computational Approach for Optimal Control Problems*. New York, NY, USA: Longman Scientific Technical, 1991.

[37] Q. Lin, R. Loxton, and K. L. Teo, "The control parameterization method for nonlinear optimal control: A survey," *J. Ind. Manage. Optim.*, vol. 10, no. 1, pp. 275–309, 2013.

[38] R. C. Loxton, K. L. Teo, V. Rehbock, and K. F. C. Yiu, "Optimal control problems with a continuous inequality constraint on the state and the control," *Automatica*, vol. 45, no. 10, pp. 2250–2257, 2009.

[39] B. Li, C. Xu, K. L. Teo, and J. Chu, "Time optimal Zermelo's navigation problem with moving and fixed obstacles," *Appl. Math. Comput.*, vol. 224, pp. 866–875, Nov. 2013.
[40] P. Liu, G. Li, and X. Liu, "Fast engineering optimization: A novel highly effective control parameterization approach for industrial dynamic processes," *ISA Trans.*, vol. 58, pp. 248–254, Sep. 2015.
[41] C. Yu, Q. Lin, R. Loxton, K. L. Teo, and G. Wang, "A hybrid time-scaling transformation for time-delay optimal control problems," *J. Optim. Theory Appl.*, vol. 169, no. 3, pp. 876–901, 2016.
[42] P. Liu *et al.*, "Control variable parameterisation with penalty approach for hypersonic vehicle reentry optimisation," *Int. J. Control*, to be published, doi: 10.1080/00207179.2018.1426882.
[43] G. Li, P. Liu, and X. Liu, "A control parameterization approach with variable time nodes for optimal control problems," *Asian J. Control*, vol. 18, no. 3, pp. 976–984, 2016.

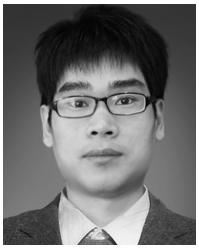

ZHIGANG REN received the M.S. degree in automatic control from the South China University of Technology, Guangzhou, China, in 2012, and the Ph.D. degree in control science and engineering from Zhejiang University, Hangzhou, China, in 2016. He is currently a Lecturer with the School of Automation, Guangdong University of Technology. His research interests include optimal control theory and applications in distributed parameter systems, robotics, and machine learning control.

ZHIJIA ZHAO received the B.Eng. degree in automatic control from the North China University of Water Resources and Electric Power, Zhengzhou, China, in 2010, and the M.S. and Ph.D. degree in automatic control from the South China University of Technology, Guangzhou, China, in 2013 and 2017, respectively. He is currently a Lecturer with the School of Mechanical and Electrical Engineering, Guangzhou University. His research interests include flexible system, ocean cybernetics, and robotics.

ZONGZE WU received the B.S. degree in material forming and control, the M.S. degree in control science and engineering, and the Ph.D. degree in pattern reorganization and intelligence system from Xi'an Jiaotong University, Xi'an, China, in 1999, 2002, and 2005, respectively. He is currently a Professor with the School of Automation, Guangdong University of Technology, Guangzhou, China. His research interests include automation control, signal processing, big data, and Internet of Things. He has served as the Under-Secretary-General for Internet of Things and Information Technology Innovation Alliance, Guangdong, China. He was a recipient of the Microsoft Fellowship Award of the MSRA in 2003, and the 2008, 2013, and 2014 recipient of the Technological Award First Prize of Guangdong Province. He was a recipient of Second Prize of Ministry of Education Technological Innovation twice, in 2012 and 2013, and the First Prize of Ministry of Education Technological Innovation in 2017.

TEHUAN CHEN received the B.S. degree from Hangzhou Dianzi University in 2011 and the Ph.D. degree from the Department of Control Science and Engineering, Zhejiang University, China, in 2016. He is currently a Lecturer with the Faculty of Mechanical Engineering and Mechanics, Ningbo University, Ningbo, China. His research interests include robotics, optimal control theory, and distributed parameter systems.